CrossMark

A study of the transmission characteristics of terahertz waves in hypersonic target flow field

Jie Zhang [1,2], **Bing Han**[1,2,†], **Shanchao Zhao**[1,2], **Guodong Zhang**[1,2] **and Wenshan Duan**[1,2]

[1]College of Physics and Electronic Engineering, Northwest Normal University, Lanzhou, 730070, PR China

[2]Engineering Research Centre of Gansu Province for Intelligent Information Technology and Application, Lanzhou Gansu, 730070, PR China

Based on the chemical reaction model proposed by Park, the 'blackout' of a reentry vehicle is studied in this paper. The temperature, pressure and electron density distribution characteristics around the reentry vehicle were simulated at various flight speeds and altitudes by USim. Subsequently, the scattering matrix method was used to study the transmission characteristics of terahertz waves in 'blackout'. The simulation results show that the temperature around the aircraft is mainly affected by speed, the pressure is mainly affected by the altitude and electron density is affected by both of these factors. The calculation results show that the transmission characteristics of terahertz waves in plasma are mainly affected by electron density, while the effects of temperature and pressure cannot be ignored either.

Key words: plasma flows, plasma sheaths, plasma simulation

1. Introduction

When a reentry vehicle reenters the atmosphere, its speed is so high that the air on the surface of the vehicle is ionized, and the ionized particles form a plasma sheath with complex composition that covers the surface of the vehicle. The plasma sheath prevents effective communication between the ground and the vehicle (Chen *et al.* 2020). So far, due to the high-pass filtering property of plasma, widely accepted has been the scheme of transmitting information by terahertz waves as carriers (Yuan *et al.* 2017; Liu *et al.* 2021). Yu *et al.* used the Wenzel–Kramers–Brillouin approximation to study the transmission characteristics of terahertz waves in plasma with different electron density distributions (Yu, Xu & Zheng 2019). Liu *et al.* constructed the Runge–Kutta exponential time finite-difference time-domain method to study the propagation characteristics of terahertz waves in cold magnetized plasma (Liu & Chao 2020). Zhou *et al.* used the shift operator finite-difference time-domain method to calculate the propagation characteristics of terahertz waves in high-temperature magnetized plasma (Zhou *et al.* 2021). Hu *et al.* proposed the scattering matrix method (SMM) based on the layered model with equal spacing, which laid a foundation for the study of the propagation characteristics of

† Email address for correspondence: 2020212189@nwnu.edu.cn

electromagnetic waves in non-uniform media (Hu, Wei & Lai 1999). Guo *et al.* assumed three different parabolic models as distribution models of electron density and collision frequency, and studied the transmission characteristics of terahertz waves in cold plasma (Guo, Guo & Li 2017). Chen *et al.* proposed a kind of improved SMM based on the SMM (Chen *et al.* 2018). These works provide theoretical support for studying the propagation of terahertz waves in inhomogeneous plasma. Insufficiently, it is subjective to express the plasma inhomogeneity by a regular mathematical model.

In order to make the calculation results more objective, the flow-field characteristics around a blunt vehicle have been simulated based on computational fluid dynamics (Bian, Li & Guo 2020; Chen *et al.* 2021) by some researchers. USim (Kundrapu *et al.* 2013; Shashurin *et al.* 2014), a professional plasma simulation software based on hydrodynamics, is developed by the Tech-X Corporation. Based on USim, Ouyang *et al.* studied the characteristics of the flow field around a blunt head and the signal loss of electromagnetic waves during reentry at different heights (Ouyang *et al.* 2019), He *et al.* studied the signal channel characteristics of terahertz waves in the flow field surrounding hypersonic vehicles (He *et al.* 2014) and Tang *et al.* sorted out and constructed a fitting model of electron density and electron collision frequency changing with flight speed, and studied and predicted the attenuation characteristics of terahertz waves at different speeds (Tang *et al.* 2019).

However, few previous works have paid attention to the transmission characteristics of terahertz waves in a realistic plasma flow field, which is mainly studied in this paper. Firstly, the simulation of the flow field around a hypersonic vehicle is completed based on USim. Secondly, the SMM is used to analyse the propagation characteristics of terahertz waves in the plasma flow field. Finally, the influence of different flight altitude and speed on the propagation characteristics of terahertz waves is discussed. The simulation model and physical model of the reentry vehicle flow field are presented in § 2. The SMM is presented in § 3. The simulation results of reentry vehicle flow field based on USim are presented in § 4. The numerical calculation results of the propagation characteristics of terahertz waves in the flow field are presented in § 5. A discussion and the significance of this study are presented in the concluding section.

2. The flow field model of reentry vehicle

In this paper, based on the Navier–Stokes equations, the simulation software USim and the model proposed by Kundrapu *et al.* (2015) are used to simulate the flow field around a hypersonic reentry vehicle. The Navier–Stokes equations are shown in (2.1)–(2.3), which are used for conservation of fluid mass, momentum and total energy, respectively:

$$\frac{\partial \rho}{\partial t} + \nabla \cdot (\rho \boldsymbol{u}) = 0, \tag{2.1}$$

$$\frac{\partial (\rho \boldsymbol{u})}{\partial t} + \nabla \cdot (\rho \boldsymbol{uu} + P\boldsymbol{I}) = \nabla \cdot \boldsymbol{\tau}, \tag{2.2}$$

$$\frac{\partial e_t}{\partial t} + \nabla \cdot (\boldsymbol{u}(e_t + \rho)) = \nabla \cdot (\boldsymbol{\tau} \cdot \boldsymbol{u}) + \nabla \cdot (\lambda \nabla T), \tag{2.3}$$

where ρ is the mass density, ∇ is the Hamiltonian, $\boldsymbol{u}$ is the velocity, $\boldsymbol{\tau}$ is the stress tensor, p is the pressure, $\boldsymbol{I}$ is the identity matrix, e_t is the total energy of the fluid which is composed of kinetic energy, chemical energy and thermal energy, λ is the thermal conductivity and T is the temperature.

The mass density can be calculated using

$$\rho = \sum_{q}^{N} n_q m_q, \tag{2.4}$$

where N is the number of components in the flow field and n_q and m_q are the particle density and mass of component q, respectively.

The pressure is defined as

$$P = \rho RT, \tag{2.5}$$

where R is the gas constant.

The stress tensor is calculated using

$$\boldsymbol{\tau} = -\frac{2}{3}\mu(\boldsymbol{\nabla} \cdot \boldsymbol{u})\boldsymbol{I} + \mu(\boldsymbol{\nabla} \cdot \boldsymbol{u} + (\boldsymbol{\nabla}\boldsymbol{u})^{T_r}), \tag{2.6}$$

where μ is the dynamic viscosity and T_r is the transpose.

The total energy is defined as

$$e_t = \frac{P}{\gamma - 1} + \frac{1}{2}\rho \boldsymbol{u} \cdot \boldsymbol{u} + \sum_{q}^{N} n_q H_q, \tag{2.7}$$

where γ is the specific thermal ratio, which is defined as $\gamma = c_p/c_v$ (c_p is specific heat at constant pressure and c_v is specific heat at constant volume), and H_q is the enthalpy of formation.

The transformation relation of each component in the flow field can be satisfied by the mass conservation expressed by (2.1). Considering (2.4) simultaneously, the density change rate s_q of each component is obtained as

$$\frac{\partial n_q}{\partial t} + \boldsymbol{\nabla} \cdot (n_q \boldsymbol{u}) = s_q. \tag{2.8}$$

Besides, other parameters of various components can be expressed as (2.9)–(2.12) according to the gas dynamics:

$$\lambda_q = \frac{5}{2}c_{v,q}\mu_q, \tag{2.9}$$

$$\mu_q = \frac{5}{16}\frac{\sqrt{\pi m_q k_b T}}{\pi \sigma^2 \Omega}, \tag{2.10}$$

$$c_{p,q} = R_q \left(\frac{d_f}{2} + 1\right), \tag{2.11}$$

$$c_{v,q} = c_{p,q} - R_q, \tag{2.12}$$

where λ_q is the fluid thermal conductivity, μ_q is viscosity, k_b is the Boltzmann constant, σ is the collision diameter, Ω is the collision integral and d_f is the number of degrees of freedom.

The RAM-C model as described by Grantham (1970), which has a length of $L = 1.295$ m, a blunt head radius of $R = 0.1524$ m and a half-cone angle of $\theta = 9°$, is used in this study. The mesh and flow-field model of the reentry vehicle are shown in figures 1(*a*)
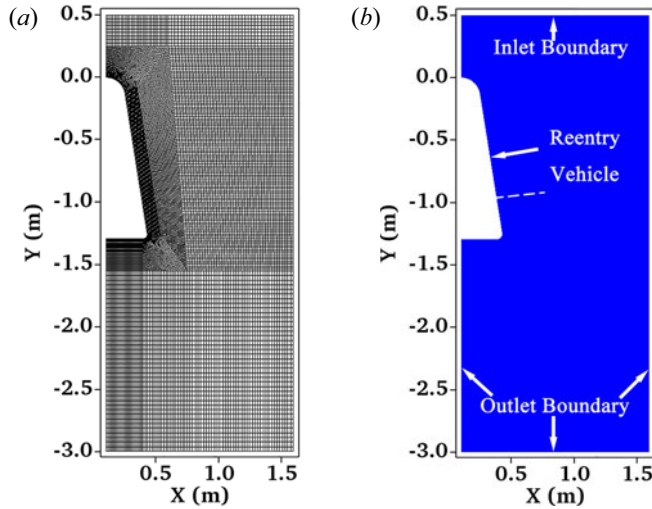
FIGURE 1. (*a*) The grid and (*b*) the initial field of the flow field around the reentry vehicle.

and 1(*b*), respectively. The incident position of the terahertz wave is represented by the dashed white line in figure 1(*b*). It is assumed that the angle of attack of free stream is 0°, so the flow field on both sides of the reentry vehicle is symmetrically distributed. Therefore, one side of the flow field is selected for study in this paper. When the altitude is 60–90 km and speed is 18–27 Ma, the air around the aircraft is in a state of thermodynamic equilibrium and chemical non-nequilibrium, the air is ionized and forms a plasma with seven components, which are N_2, O_2, NO, N, O, NO^+ and e (electrons) (Le 2005). Seven components and eighteen chemical reactions proposed by Park were used in this study (Park 1985*a*, 1985*b*).

3. The propagation models of terahertz waves

The SMM (Hu *et al.* 1999; Guo *et al.* 2017) is used to analyse the transmission characteristics of terahertz waves in 'blackout'. The propagation model of terahertz waves in plasma is shown in figure 2. The boundary of the plasma layer is assumed to be flat, and the plasma sheath is divided into some parallel sublayers equally. The plasma properties among these sublayers are different, but the internal property of each layer is uniform. For better transmission efficiency, it is assumed that the terahertz wave is incident perpendicularly into the plasma sheath. According to figure 2, both incident and reflected waves exist in the incident region (0), and the total electric field can be described as

$$E_{z,0} = E_0(e^{-jk_0 z} + A\,e^{jk_0 z}), \tag{3.1}$$

the total electric field in each sublayer plasma is described as

$$E_{z,i} = E_0(B_i\,e^{-jk_i z} + C_i\,e^{jk_i z}), \tag{3.2}$$

there is only transmitted wave but no reflected wave in the transmitted region ($n+1$) and the total field is described as

$$E_{z,n+1} = E_0 D\,e^{-jk_{n+1}z}, \tag{3.3}$$

where the total reflection coefficient and the total transmission coefficient are represented by A and D, respectively. The transmission and reflection coefficients in the *i*th-layer
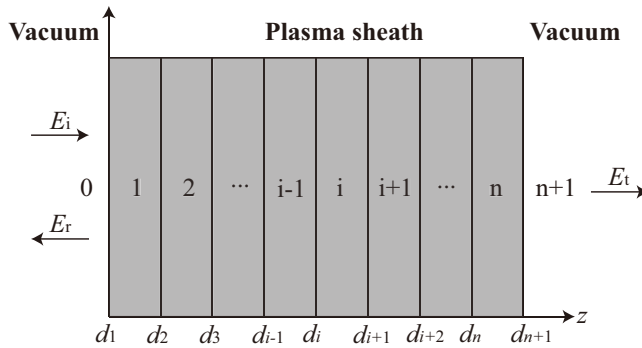
FIGURE 2. Schematic diagram of the SMM.

plasma are represented by B_i and C_i, respectively. In addition, $k_i = k_0\sqrt{\varepsilon_{r,i}}$ is the wavenumber of terahertz wave transmission in the ith-layer plasma. Therein, $k_0 = \omega\sqrt{\mu_0\varepsilon_0} = \omega/c$, $\mu_0 = 4\pi \times 10^{-7}$ H·m^{-1} is the permeability in vacuum and $c = 3 \times 10^8$ m·s^{-1} is the speed of light in vacuum.

According to the formula deduced by Heald, Wharton & Furth (1965), the relative permittivity of plasma is approximately expressed as

$$\varepsilon_{r,i} = \left(1 - \frac{\omega_{p,i}^2}{\omega^2 + v_{e,i}^2}\right) - j\frac{v_{e,i}}{\omega}\frac{\omega_{p,i}^2}{\omega^2 + v_{e,i}^2}, \qquad (3.4)$$

where the angular frequency of the particles in the plasma is lower than the angular frequency of the electrons, and it can be deduced that $\omega_p \approx \omega_{pe} = \sqrt{N_e e^2/\varepsilon_0 m_e}$. Here N_e is the electron density in the plasma sheath, $e = 1.602 \times 10^{-19}$ C is the electron charge, $\varepsilon_0 = 8.854 \times 10^{-12}$ F·m^{-1} is the dielectric constant in vacuum and $m_e = 9.109 \times 10^{-31}$ kg is the electron mass. Parameter $v_e = 5.82 \times 10^{12} P/\sqrt{T}$ is the collision frequency of electrons in the plasma (Ouyang *et al.* 2021), which is obviously dependent on the temperature T and pressure P of the plasma sheath.

According to the boundary conditions of continuous matching of electric field, the coefficient transformation relationship between adjacent plasma layers can be shown to be

$$\begin{pmatrix} B_i \\ C_i \end{pmatrix} = \mathbf{S}_i \begin{pmatrix} B_{i-1} \\ C_{i-1} \end{pmatrix}. \qquad (3.5)$$

The scattering matrix $\mathbf{S}_i$ in the ith-layer plasma is expressed as

$$\mathbf{S}_i = \begin{pmatrix} e^{-jk_i d_i} & e^{jk_i d_i} \\ k_i\, e^{-jk_i d_i} & -k_i\, e^{-jk_i d_i} \end{pmatrix}^{-1}$$
$$\times \begin{pmatrix} e^{-jk_{i-1} d_{i-1}} & e^{jk_{i-1} d_{i-1}} \\ k_{i-1}\, e^{-jk_{i-1} d_{i-1}} & -k_{i-1}\, e^{-jk_{i-1} d_{i-1}} \end{pmatrix}. \qquad (3.6)$$

The relation between the total incidence field and the total transmission field is expressed as

$$\mathbf{S}_g \begin{pmatrix} A \\ 1 \end{pmatrix} = \mathbf{V}D, \qquad (3.7)$$

Altitude (km)	Temperature (K)	Pressure (Pa)	Density (kg $\cdot$ m^{-3})
51	294.38	75.58	8.95×10^{-4}
61	324.28	25.12	2.70×10^{-4}
71	354.18	9.20	9.05×10^{-5}

TABLE 1. The maximum temperature, pressure and density of the atmosphere at different altitudes.

where

$$V = \frac{1}{2k_n} \begin{pmatrix} k_n + k_{n+1} e^{j(k_n - k_{n+1})d_p} \\ k_n - k_{n+1} e^{-j(k_n + k_{n+1})d_p} \end{pmatrix}. \tag{3.8}$$

Here S_g is the global scattering matrix, which can also be described as

$$S_g = \left(\prod_{i=n}^{2} S_i \right) S_1. \tag{3.9}$$

By transforming S_g into (S_{g1}, S_{g2}), (3.7) is derived as

$$\begin{pmatrix} A \\ D \end{pmatrix} = - \begin{pmatrix} S_{g1} & -V \end{pmatrix}^{-1} S_{g2}. \tag{3.10}$$

The reflection coefficient A and transmission coefficient D are calculated. And further, the transmissivity, reflectivity and absorptivity can be expressed by

$$\begin{cases} \Gamma_t = |A|^2, \\ T_t = |D|^2, \\ A_t = 1 - \Gamma_t - T_t, \end{cases} \tag{3.11}$$

where Γ_t is the total reflectivity of the plasma sheath to terahertz waves, T_t is the total transmittivity of terahertz waves through the plasma sheath and A_t is the total absorptivity of terahertz waves by the plasma sheath.

4. Simulation and analysis

The flow field characteristics of the reentry vehicle surface at different flight altitudes (H) and speeds (V) are analysed in this simulation. The temperature and density of the atmosphere vary with altitude (NASA, Glenn Research Center 2021). According to the formula of atmospheric properties, the data of atmospheric temperature, pressure and density for different altitudes are shown in table 1.

The simulation of plasma flow field around a blunt reentry vehicle was analysed using Tech-X USim. The simulation results are shown in figures 3 and 4. It is obvious that the free stream covers the blunt head with a sheath much larger than the blunt head due to the hypersonic characteristic of the reentry vehicle. The sheath around the head of the reentry vehicle has higher pressure, temperature and electron density; these three parameters are smaller at the tail of the blunt head. That is why the reentry antenna is installed at the tail of the blunt head. In order to further study the influence of external conditions on the internal characteristics of the flow field, the values of peak temperature and peak pressure for different conditions are shown by the dots in figure 5 based on figures 3 and 4. As
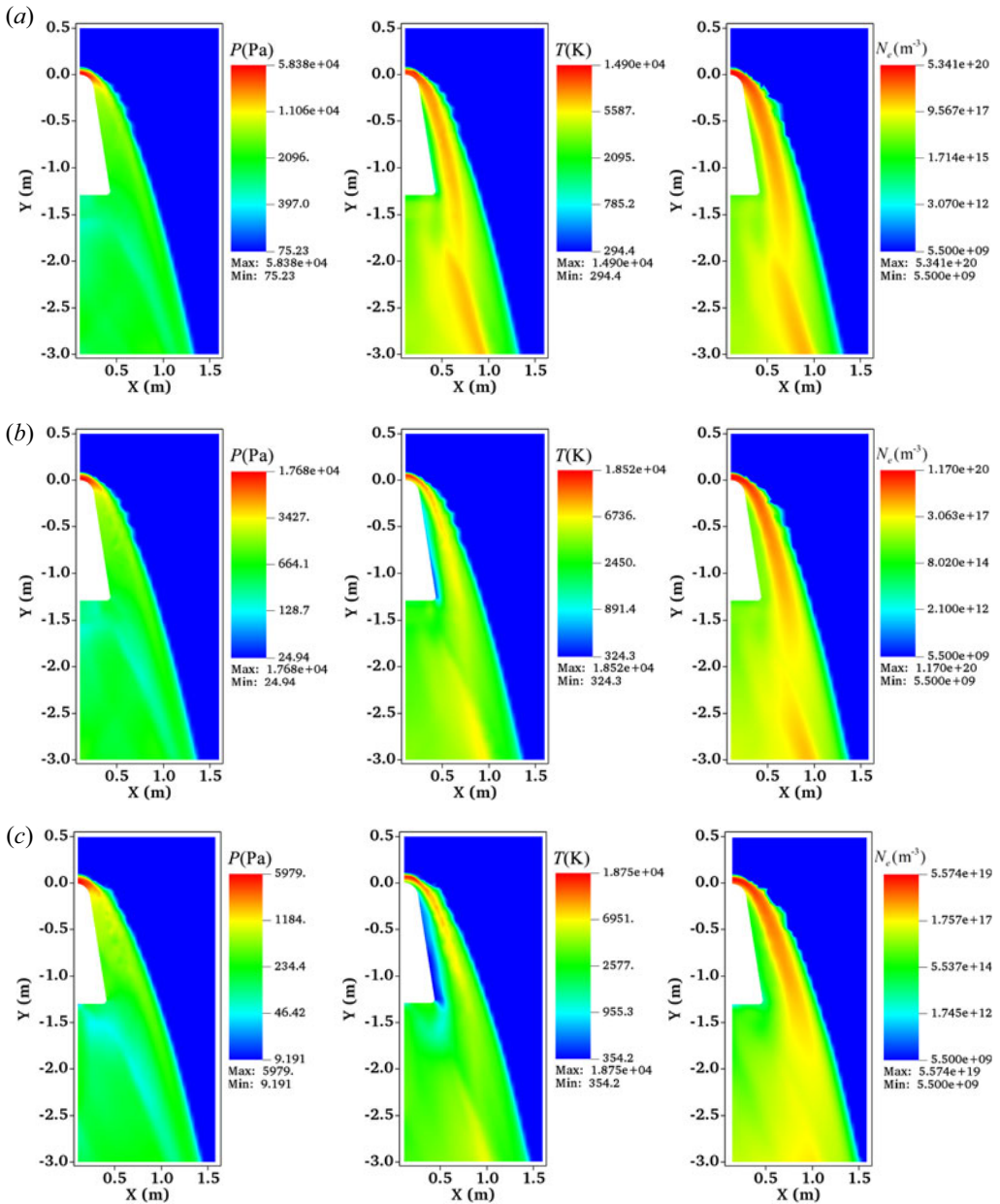
FIGURE 3. Flow-field distribution around the reentry model at a speed of 25 Ma for different flight altitudes: (*a*) 51 km, (*b*) 61 km and (*c*) 71 km.

shown in figure 5(*a*), with an increase of altitude, it can be seen that the temperature increases significantly at 51–61 km and then decreases slightly at 61–71 km. As shown in figure 5(*b*), with an increase of speed, it can be seen that the changes of temperature and pressure are relatively stable for 23–25 and 25–27 Ma.

The simulation results and table 1 show that with an increase of flight altitude, the decrease of free-stream density is the main reason for the decrease of electron density.
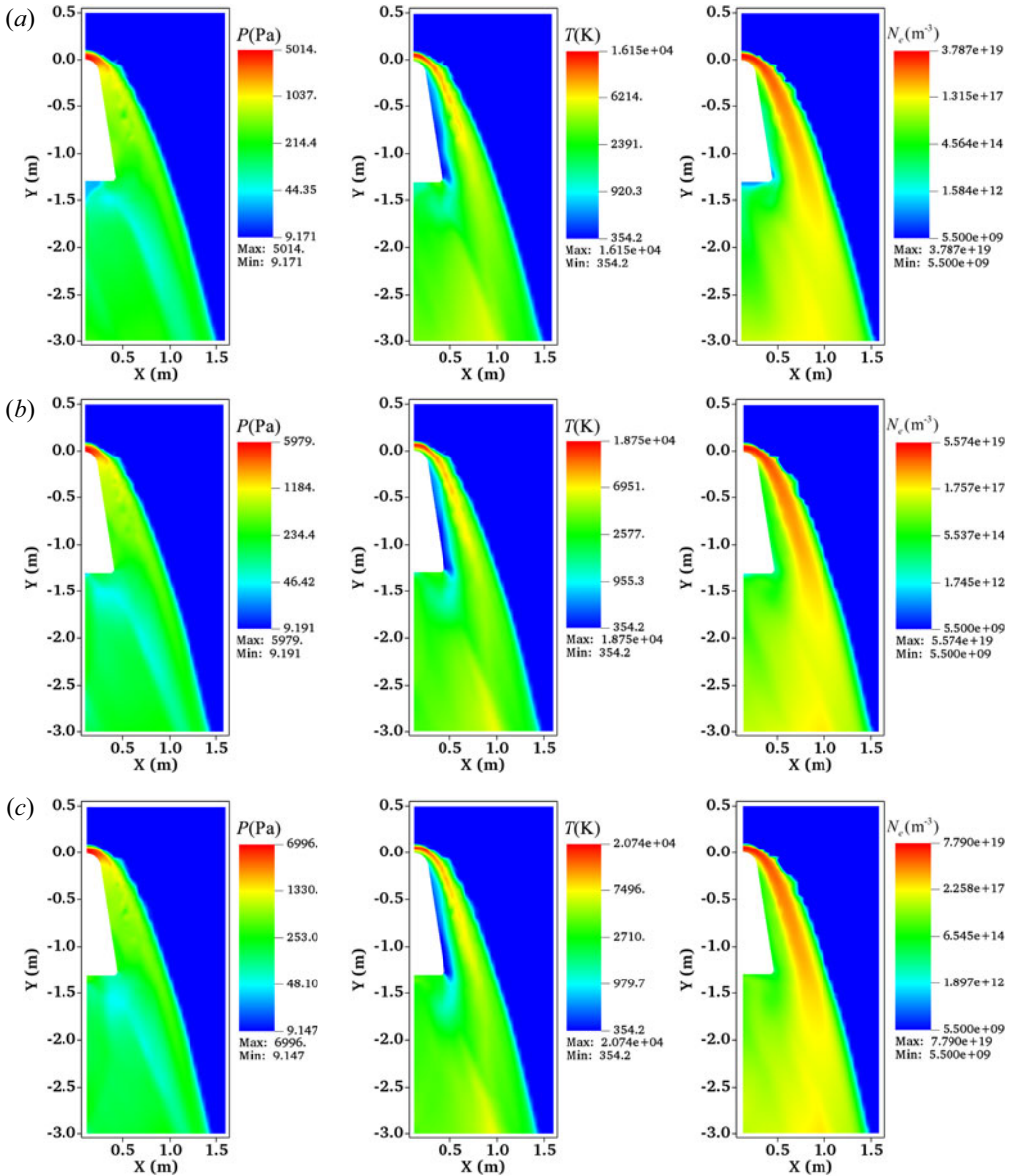
FIGURE 4. Flow-field distribution around the reentry model at an altitude of 71 km for different flight speeds: (*a*) 23 Ma, (*b*) 25 Ma and (*c*) 27 Ma.

With an increase of speed, the temperature of the flow field increases significantly, which promotes the efficiency of electron generation and indirectly increases electron density.

5. Calculation results and discussion

In this section, the parameters of the numerical calculation are assumed to be that the transmission frequency of the terahertz wave is 0.1–1.0 THz, the flight altitude is 51–71 km and the flight speed is 21–27 Ma. The oscillation characteristics of reflectivity are scaled in decibels.
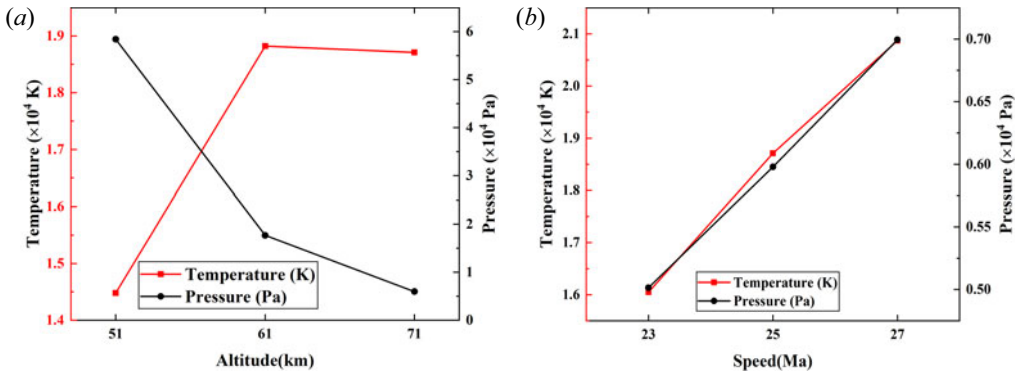
FIGURE 5. The maximum temperature and maximum pressure for different flow-field conditions. (*a*) The flight speed is 25 Ma. (*b*) The flight altitude is 71 km.
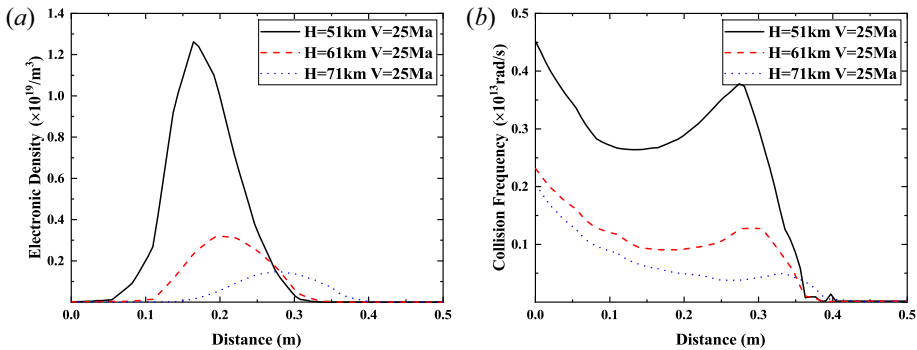

FIGURE 6. The electron characteristics of plasma for different altitudes. (*a*) Electron density. (*b*) Electron collision frequency.

5.1. *Influence of altitude*

According to figure 3, the distributions of electron density and electron collision frequency at the tail of the blunt reentry vehicle vary with altitude, as shown in figure 6. It can be seen that the electron density is very low, but the electron collision frequency is very high at the surface of the vehicle. With an increase of altitude, the electron density decreases and the peak position moves gradually away from the aircraft surface from 0.2 to 0.3 m; the electron collision frequency decreases and the peak position moves gradually away from the surface of the aircraft from 0.3 to 0.35 m.

It is shown in figure 7 that the transmission characteristics of terahertz waves in the flow field around the reentry vehicle vary with altitude. It can be seen that the transmissivity decreases with a decrease of altitude, while the reflectivity and absorptivity increase with a decrease of altitude. Physically speaking, a decrease in altitude leads to an increase in atmospheric pressure and temperature, which makes electrons in the plasma collide more frequently. At the same time, the increase of free-stream density in the flow field makes more particles participate in the thermochemical reaction around the reentry vehicle, resulting in an increase of electrons in the reaction products and the electron density in the flow field is increased. A large number of electrons weaken the energy in the terahertz waves, which is manifested as the absorptivity of the plasma sheath to the terahertz waves being increased, and the transmissivity of the terahertz waves in the plasma is decreased.
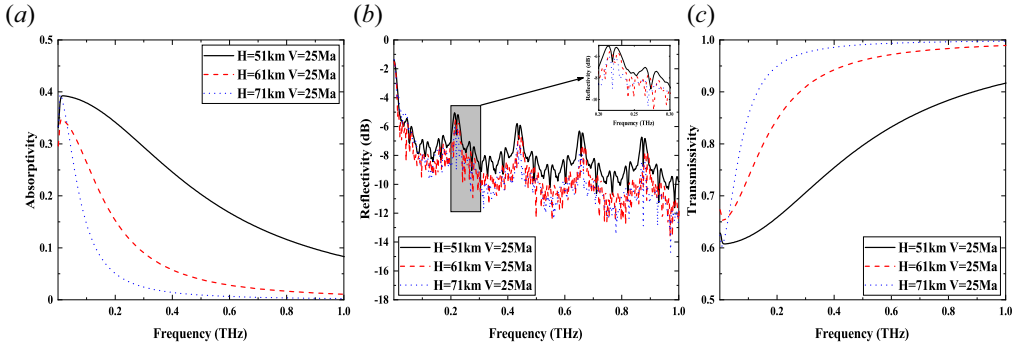
FIGURE 7. The transmission characteristics of terahertz waves for different altitudes. (*a*) Transmissivity. (*b*) Reflectivity. (*c*) Absorptivity.
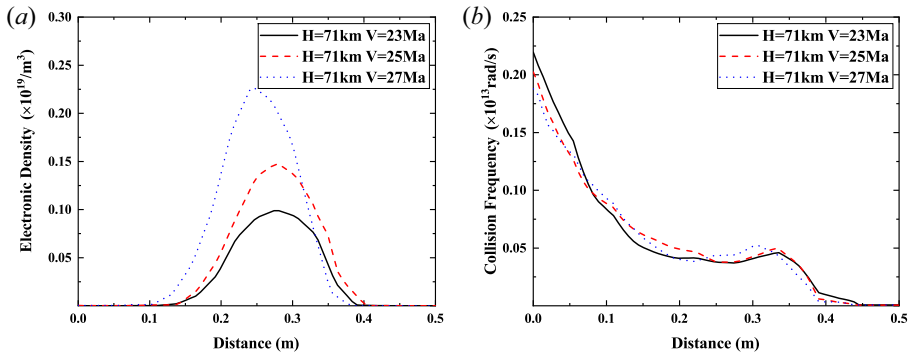

FIGURE 8. The electron characteristics of plasma for different flight speeds. (*a*) Electron density. (*b*) Electron collision frequency.

5.2. *Influence of flight speed*

According to figure 4, the distributions of electron density and electron collision frequency at the tail of the blunt reentry vehicle vary with flight speed, as shown in figure 8. It can be seen that, with an increase of speed, the peak electron density increases and the peak position gradually approaches the aircraft surface from 0.3 to 0.25 m, but the curve of electron collision frequency remains basically unchanged.

It is shown in figure 9 that the transmission characteristics of terahertz waves in the flow field around the reentry vehicle vary with speed. It can be seen that the transmittance decreases with an increase of speed, while reflectivity and absorptivity increase with an increase of speed. Physically speaking, with an increase of flight speed, the kinetic energy of particles in the flow field increases, which is macroscopically manifested as an increase of flow-field temperature. It transforms the ordered kinetic energy into disordered kinetic energy among particles and reduces the effective collision frequency of electrons. The energy of the terahertz wave is consumed by the electrons with low collision frequency, which leads to an increase of absorptivity of the terahertz wave by the plasma. Meanwhile, the increase of flow-field temperature can promote the thermochemical reaction in the flow field, and improve the electron generation efficiency of the thermochemical reaction. As the electron density in the plasma is increased, the transmittance is decreased and the reflectivity is increased.
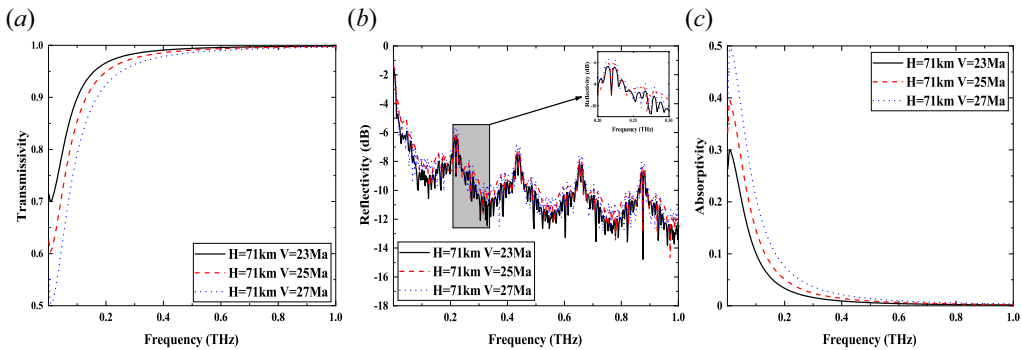
FIGURE 9. The transmission characteristics of terahertz waves for different flight speeds. (*a*) Transmissivity. (*b*) Reflectivity. (*c*) Absorptivity.

6. Summary and conclusion

In this paper, the transmission characteristics of terahertz waves in hypersonic target flow field are studied. Firstly, the control variable method is used to simulate the flow-field distribution around the RAM-C reentry vehicle at different altitudes and speeds. Secondly, the variation of electron density and electron collision frequency in the flow field is analysed according to the simulation results. Finally, the SMM is used to study the propagation characteristics of terahertz waves in the hypersonic reentry flow field under different conditions. The results show that, with a decrease of altitude, the electron density increases with an increase of air density and the electron collision frequency increases with an increase of air pressure. In addition, with an increase of speed, the increase of flow-field temperature increases the electron density and electron collision frequency. In both cases, the absorptivity of the plasma sheath to terahertz waves increases, so that the transmission capacity of terahertz waves in the plasma flow field is weakened. The study provides some reference for mathematical modelling and theoretical analysis of electron density and electron collision frequency in 'blackout'.

Declaration of interest

The authors report no conflict of interest.

Appendix A

The atmospheric properties at different altitudes (*H*), which is in units of km, are expressed as follows (NASA, Glenn Research Center 2021). The temperature of the

atmosphere (in K) is

$$T = 273.1 + \begin{cases} -131.21 + 2.99H & H > 25 \\ -56.46 & 11 \le H \le 25 \\ 15.04 - 6.49H & 0 \le H < 11 \end{cases} \tag{A1}$$

The pressure of the atmosphere (in Pa) is

$$P = \begin{cases} 2.49 \times 10^3 \left(\dfrac{T}{216.6}\right)^{-11.39} & H > 25 \\ 2.27 \times 10^4 \exp(1.73 - 0.16H) & 11 \le H \le 25 \\ 1.01 \times 10^3 \left(\dfrac{T}{288.06}\right)^{5.26} & 0 \le H < 11 \end{cases} \tag{A2}$$

The density of the atmosphere (in $kg \cdot m^{-3}$) is

$$\rho = 3.49 \times 10^{-3} \frac{P}{T}. \tag{A3}$$

REFERENCES

BIAN, Z., LI, J. & GUO, L. 2020 Simulation and feature extraction of the dynamic electromagnetic scattering of a hypersonic vehicle covered with plasma sheath. *J Remote Sens*. **12** (17), 2740.

CHEN, X., SHEN, F., LIU, Y., AI, W. & LI, X. 2018 Improved scattering-matrix method and its application to analysis of electromagnetic wave reflected by reentry plasma sheath. *IEEE Trans. Plasma Sci*. **46** (5), 1755–1767.

CHEN, K, XU, D, LI, J, GENG, X, ZHONG, K & YAO, J 2020 Propagation characteristics of terahertz wave in hypersonic plasma sheath considering high temperature air chemical reactions. *Optik* **208** (208), 164090.

CHEN, K., XU, D., LI, J., ZHONG, K. & YAO, J. 2021 Studies on the propagation properties of thz wave in inhomogeneous dusty plasma sheath considering scattering process. *Results Phys*. **24**, 104109.

GRANTHAM, W.L. 1970 Flight results of a 25000-foot-per-second reentry experiment using microwave reflectometers to measure plasma electron density and standoff distance. *Tech. Rep*. NASA TN D-6062.

GUO, L., GUO, L. & LI, J.. 2017 Propagation of terahertz electromagnetic waves in a magnetized plasma with inhomogeneous electron density and collision frequency. *Phys. Plasmas* **24** (2), 022108.

HE, G., ZHAN, Y., GE, N., PEI, Y., WU, B. & ZHAO, Y. 2014 Channel characterization and finite-state markov channel modeling for time-varying plasma sheath surrounding hypersonic vehicles. *Prog. Electromag. Res*. **145**, 299–308.

HEALD, M.A., WHARTON, C.B. & FURTH, H.P. 1965 Plasma diagnostics with microwaves. *Phys. Today* **18** (9), 72–74.

HU, B.J., WEI, G. & LAI, S.L. 1999 Smm analysis of reflection, absorption, and transmission from nonuniform magnetized plasma slab. *IEEE Trans. Plasma Sci*. **27** (4), 1131–1136.

KUNDRAPU, M., LOVERICH, J., BECKWITH, K., STOLTZ, P., SHASHURIN, A. & KEIDAR, M. 2015 Modeling radio communication blackout and blackout mitigation in hypersonic vehicles. *J. Spacecr. Rockets* **52** (3), 853–862.

KUNDRAPU, M., LOVERICH, J., BECKWITH, K., STOLTZ, P. & ZHUANG, T. 2013 Modeling and simulation of weakly ionized plasmas using nautilus. *51st AIAA Aerospace Sciences Meeting including the New Horizons Forum and Aerospace Exposition*, AIAA-2013-1187. doi: 10.2514/6.2013-1187.

LE, J.L. 2005 *Reentry Physics*, pp. 15–21. National Defense Industry Press.

LIU, H.Y. & CHAO, Y. 2020 Research on terahertz band electromagnetic characteristics of propagation and scattering in the cold magnetized plasma medium. *Optik* **217**, 164905.

LIU, J. X., ZHAO, Y., LV, J. J. & QU, S. 2021 Thz wave propagation in the stagnation region of reentry plasma sheath. *AIP Adv.* **11** (6), 065001.

NASA, GLENN RESEARCH CENTER 2021 Earth atmosphere model. Available at: https://www.grc.nasa.gov/WWW/K-12/airplane/atmosmet.html.

OUYANG, W., JIN, T., WU, Z. & DENG, W. 2021 Study of terahertz wave propagation in realistic plasma sheath for the whole reentry process. *IEEE Transactions on Plasma Science* **49** (1), 460–465.

OUYANG, W., LIU, Y., DENG, W., ZHANG, Z. & ZHAO, C. 2019 Study of the electromagnetic wave propagation in realistic plasma. *J. Microwave Opt. Technol. Lett.* **62** (7), 1–9.

PARK, C. 1985a On convergence of computation of chemical reacting flows. *AIAA 23rd Aerospace Sciences Meeting*, AIAA-85-0247. doi: 10.2514/6.1985-247.

PARK, C. 1985b Problems of rate chemistry in the flight regimes of aeroassisted orbital transfer vehicles. *AIAA 19th Thermophysics Conference*, AIAA-84-1730. doi: 10.2514/6.1984-1730.

SHASHURIN, A., ZHUANG, T., TEEL, G., KEIDAR, M., KUNDRAPU, M., LOVERICH, J., BEILIS, I.I. & RAITSES, Y. 2014 Laboratory modeling of the plasma layer at hypersonic flight. *J. Spacecr. Rockets* **51** (3), 838–846.

TANG, R., MAO, M., YUAN, K., WANG, Y. & DENG, X. 2019 A terahertz signal propagation model in hypersonic plasma sheath with different flight speed. *J. Phys. Plasmas* **26** (4), 043509.

YU, H., XU, G. & ZHENG, Z. 2019 Transmission characteristics of terahertz waves propagation in magnetized plasma using the WKB method. *Optik* **188**, 244–250.

YUAN, K., WANG, Y., SHEN, L., YAO, M., DENG, X., ZHOU, F. & CHEN, Z. 2017 Sub-thz signals' propagation model in hypersonic plasma sheath under different atmospheric conditions. *Sci. China* **60** (11), 113301.

ZHOU, Z., WAN, X., LI, X., ZHANG, J., ZHOU, Y., REN, X. & SHI, Y. 2021 So-FDTD analysis on transmission characteristics of terahertz wave in plasma. *Phys. Plasmas* **28** (7), 072105.